

Harmonic and single pulse operation of a Raman laser using graphene

This article has been downloaded from IOPscience. Please scroll down to see the full text article.

2012 Laser Phys. Lett. 9 223

(<http://iopscience.iop.org/1612-202X/9/3/008>)

View [the table of contents for this issue](#), or go to the [journal homepage](#) for more

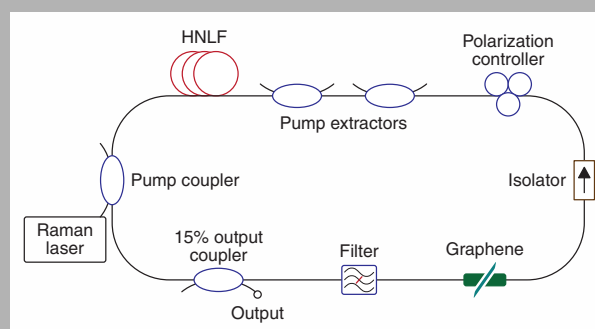
Download details:

IP Address: 155.198.206.210

The article was downloaded on 16/04/2013 at 19:45

Please note that [terms and conditions apply](#).

Abstract: We present an all-fiber passively mode-locked Raman laser using graphene as a saturable absorber. Different lengths of a highly non-linear fiber presenting normal dispersion at both pump and signal wavelengths are used in the cavity to provide Raman amplification. The cavity is pumped by a continuous wave Raman laser at 1450 nm, and generates short pulses around 1550 nm, which depending on polarization and filtering parameters can be either at the repetition rate of the cavity or at higher harmonics of it.



Raman oscillator configuration. HNLF – highly nonlinear fiber

© 2012 by Astro Ltd.

Published exclusively by WILEY-VCH Verlag GmbH & Co. KGaA

Harmonic and single pulse operation of a Raman laser using graphene

C.E.S. Castellani,^{1,*} E.J.R. Kelleher,¹ Z. Luo,² K. Wu,³ C. Ouyang,³ P.P. Shum,^{3,4} Z. Shen,² S.V. Popov,¹ and J.R. Taylor¹

¹Femtosecond Optics Group, Department of Physics, Blackett Laboratory, Prince Consort Road, Imperial College London, London SW7 2AZ, UK

²Division of Physics and Applied Physics, School of Physical and Mathematical Sciences, Nanyang Technological University, Singapore 637371, Singapore

³School of Electrical and Electronic Engineering, Nanyang Technological University, Singapore 637553, Singapore

⁴CINTRA CNRS/NTU/THALES, UMI 3288, Research Techno Plaza, 50, Nanyang Drive, Border X Block, Level 6, Singapore 637553, Singapore

Received: 3 November 2011, Revised: 4 November 2011, Accepted: 7 November 2011

Published online: 16 January 2012

Key words: Raman laser; mode-locking, graphene

1. Introduction

Raman fiber lasers present additional unique characteristics that usually cannot be obtained with rare earth doped fibers as the lasing medium. The most significant is versatility in terms of wavelength, since Raman gain is achievable throughout the complete window of transparency of silica (300–2200 nm). Providing that a suitable high power pump is provided, the Raman amplification process can be cascaded several times [1] allowing lasing in a broad wavelength range. Such wavelength versatility cannot be achieved using traditional lasers based on rare-

earth-doping that have limited emission bands not broader than a few tens of nanometers.

This concept of wavelength versatility is also valid for short-pulsed laser sources, such as mode-locked lasers. Mode-locking is a widely deployed technique that allows an extensive range of pulse durations and energies to be achieved in fiber lasers [2–6]. More specifically, mode-locked lasers can take advantage of Raman amplification to provide picosecond or sub-picosecond pulses at non-conventional wavelengths. A number of mode-locked Raman lasers have already been reported [7–10] using techniques such as the figure-of-eight geometry [7] dissipative four-wave-mixing [8] and semiconductor saturable ab-

* Corresponding author: e-mail: c.schmidt-castellani09@imperial.ac.uk

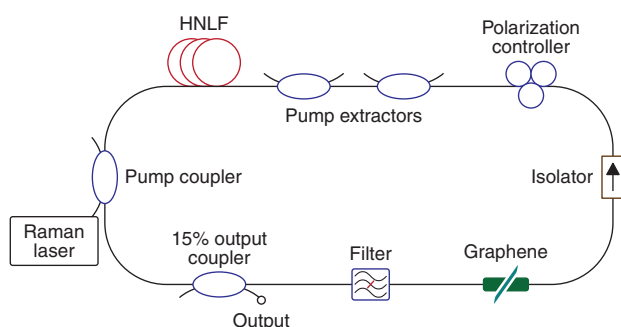


Figure 1 (online color at www.lphys.org) Raman oscillator configuration. HNLF – highly nonlinear fiber

sorber mirrors (SESAM) [10]. However, in order to fully exploit the wavelength versatility of Raman amplification with a reliable and environmentally stable technique, a single broadband non-wavelength-specific saturable absorber is required.

Carbon nanotubes [11–13] can be a partial solution to this problem since they can provide saturable absorption across a broad wavelength range due to the fact that it is possible to have nanotubes with a large variety of diameters embedded in a single device. As an example, in [11] a single sample of carbon nanotubes was used as a mode-locking device over the broad wavelength range from around 1 to 2 μm . This technique of combining Raman amplification and carbon nanotubes was experimentally demonstrated at the wavelengths of 1120 and 1660 nm [14,15].

Notwithstanding, the recent development of graphene technology [16–19] has opened the possibility of a more universal solution since graphenes saturable absorption is virtually wavelength independent and therefore it can be used as a mode-locking device across the whole silica transparency window, which in combination with Raman gain can produce a fully versatile wavelength independent technique to mode-lock fiber lasers. Here we present a Raman laser mode-locked by a 4–5 layers graphene in the dissipative soliton regime [20–24] generating hundreds of picosecond pulses around 1550 nm.

2. Experimental setup

The laser set-up is shown in Fig. 1. It consists of an all-fiber optical cavity pumped by a high power continuous wave (CW) Raman laser at 1450 nm in a counter-propagating configuration. The optical fibers used as the Raman gain medium were different lengths of a single-mode speciality optical fiber (OFS Raman fiber), with an enhanced germanium oxide (GeO_2) concentration for an increased Raman gain coefficient ($2.5 \text{ W}^{-1}\text{km}^{-1}$). The fibers dispersion at 1550 nm was -20.5 ps/nm/km with

a slope of $0.031 \text{ ps/nm}^2/\text{km}$ and effective core area of $18.6 \mu\text{m}^2$. Two wavelength division multiplexing (WDM) couplers were used after the fiber in order to dump the residual pump power out of the cavity, which otherwise could have damaged the optical components of the oscillator. A polarization insensitive optical isolator was employed to ensure unidirectional propagation and a 15% output coupler was used. The graphene saturable absorber was introduced into the cavity through transferring a piece of free standing few layers graphene film onto the end facet of a fiber pigtail *via* the Van der Waals force [25,26], and an intra-cavity polarization controller allowed fine adjustment of the cavity birefringence. An optical filter with variable bandwidth was used to assist the intra-cavity pulse shaping dynamics. The insertion loss of the graphene was measured to be around 0.4 dB in the range from 1520 to 1580 nm.

3. Results

The initial results were obtained using a length of 100 m non-linear fiber. In this configuration no optical filter was employed in the cavity since the fiber gain length was insufficient to overcome the filter insertion loss of 3 dB. The mode-locking threshold was achieved under 4.4 W pump power, and pulsed operation was maintained up to the maximum power of the pump source of 4.8 W. For pumping with 4.8 W, the oscilloscope trace, the optical spectrum and the electrical or radio frequency (RF) spectrum at the cavity output are shown in Fig. 2. The generated pulses were 750 ps long with an average power of 8.3 mW. The spectrum has a linewidth of 1.6 nm at 6 dB and a square shape typical of lasers operating in the dissipative soliton regime. The pulses were generated at a repetition rate of 315.96 MHz, which is approximately 160 times the repetition rate of a single pulse operation in a 100 m long optical cavity. Harmonic mode-locking is likely to happen when a saturable absorber with weak absorption is used, which normally should be the case for a few layers of graphene interface [27]. Moreover, since Raman amplification is effectively instantaneous, no energy can be stored; therefore gain is available all the time making pulses likely to build up more than once per round trip.

By changing the polarization and the pump power, strong long-term modulations could be observed in the pulse train as well as changes in the spectral and temporal pulse shape. However the associated change in the repetition rate was no more than 10%. We believe the absence of a wavelength restrictive filter meant the pulse train could not remain stable over a period of time greater than 15–20 minutes. Using a 100-m length fiber, operation with a single pulse per round trip was not achieved.

Increasing the fiber length to 200 m decreased the threshold level to 2.6 W, and again pulsed output was obtained over the available pump power range. Using the maximum pump power of 4.8 W and a 4.8 nm bandwidth

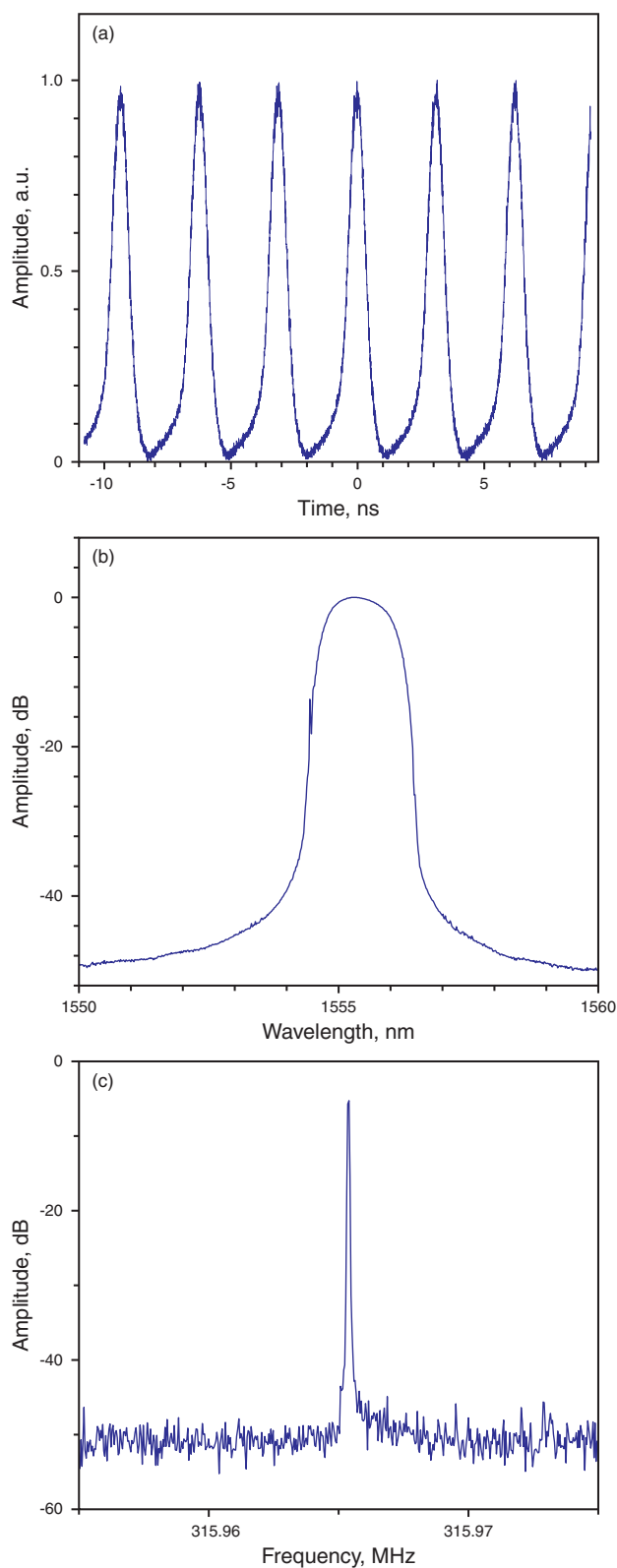


Figure 2 (online color at www.lphys.org) (a) – oscilloscope temporal trace of the high harmonic mode-locked 750 ps pulses from the cavity without filter and with 100 m of non-linear fiber, (b) – optical spectrum, and (c) – RF trace

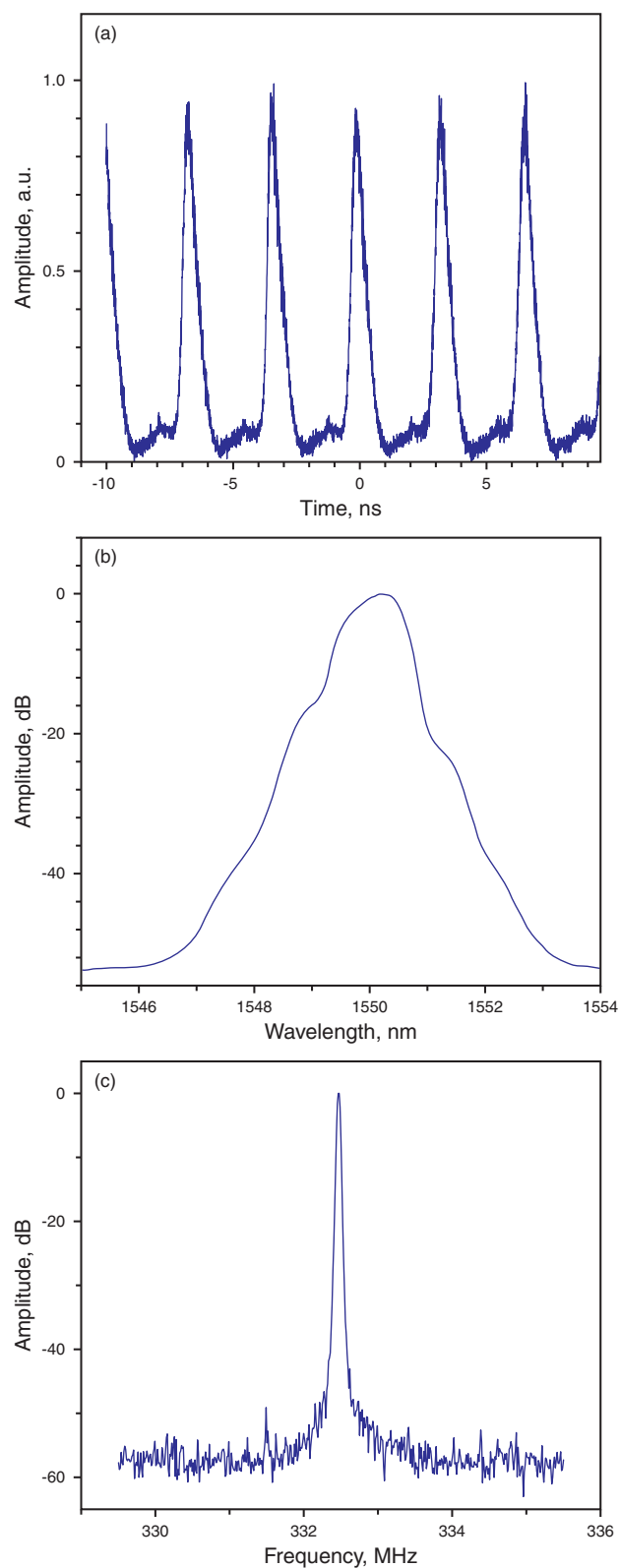


Figure 3 (online color at www.lphys.org) (a) – oscilloscope temporal trace of the high harmonic mode-locked 600 ps pulses from the cavity with spectral filtering and with 200 m of non-linear fiber, (b) – optical spectrum, and (c) – RF trace

filter centered at 1550 nm resulted in a train of 600 ps pulses with 332.5 MHz repetition rate and 8.5 mW average power as can be seen in Fig. 3. The spectrum has a squared shape top with a 6 dB level bandwidth of 1.2 nm; however a substantial pedestal component was present. In this configuration the laser was not strongly affected by changes of polarization and pump power, and the pulses and spectral shapes remained unchanged over a period of hours of operation. We attribute this higher stability to the use of the optical filter in the cavity, which is necessary for mode-locking in the dissipative soliton regime as the other elements of the cavity do not provide sufficient spectral filtering. The repetition rate exhibited little variation, remaining within a few discrete values between 310 and 340 MHz.

Other filters with 12.8, 2.3, and 1.0 nm bandwidths were also tested with the center wavelength varying in the range from 1540 to 1560 nm. Apart from changes in the spectral shape, single pulse per round trip mode-locking was not observed and pulsed output was always in high harmonics of the cavity with insignificant variations of the pulse parameters and repetition rate. However, when the filter was removed a single pulse per round trip operation could be achieved, which is shown in Fig. 4. This operational regime was obtained for pump powers just above the threshold. Further increase of the pump power caused pulse break down and higher harmonic mode-locking.

The main cavity harmonic mode-locked pulses were 1.25 ns long, with an output average power of 4.9 mW at 0.9 MHz repetition rate, corresponding to the round trip time of the cavity. The longer pulse duration was mainly due to the absence of an optical filter and the longer length of fiber, which were also sources of instability, making the single pulse operation difficult to maintain for more than a few minutes. The spectrum had a Gaussian-like shape with a 6 dB bandwidth of 0.8 nm and the RF trace had a contrast of approximately 50 dB against the noise floor.

Increasing the fiber length to 400 m leads to harmonic mode-locking with pulse durations from 600 to 700 ps and repetition rates from 310 to 340 MHz, depending on pump power, filter bandwidth, central wavelength and polarization adjustment. Single pulse operation could only be achieved when a filter with a bandwidth of 12.8 nm was used. This time the pulse duration was 600 ps and the average power 3.3 mW, achieved when the cavity was pumped with 2.8 W power. The repetition rate of 500 kHz, matched exactly the cavity round trip, and the spectral 6 dB level bandwidth was 0.6 nm. Within the pump powers from threshold to approximately 25% higher, the single pulse regime could be maintained and exhibited significantly higher stability than that obtained with the previous setup, without an optical filter.

In order to confirm the chirped nature of the pulse, a signature of dissipative solitons, a 21 km length of a standard Telecom fiber (STF) was spliced to the cavity output providing anomalous dispersion to compensate the expected positive chirp on the pulses. Given the narrow spectral bandwidth (0.6 nm) and the large duration (600 ps), the

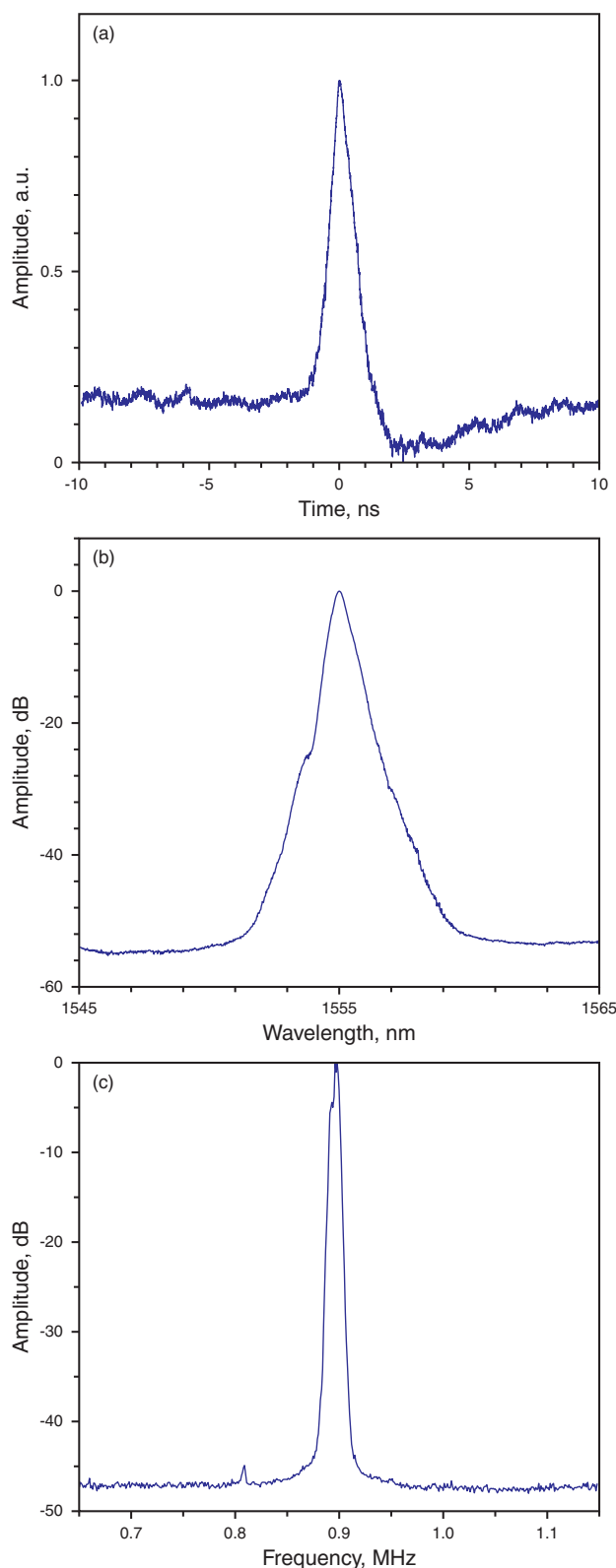


Figure 4 (online color at www.lphys.org) (a) – oscilloscope trace of the single-pulses mode-locked cavity without filter and with 200 m of non-linear fiber, (b) – optical spectrum, and (c) – RF trace

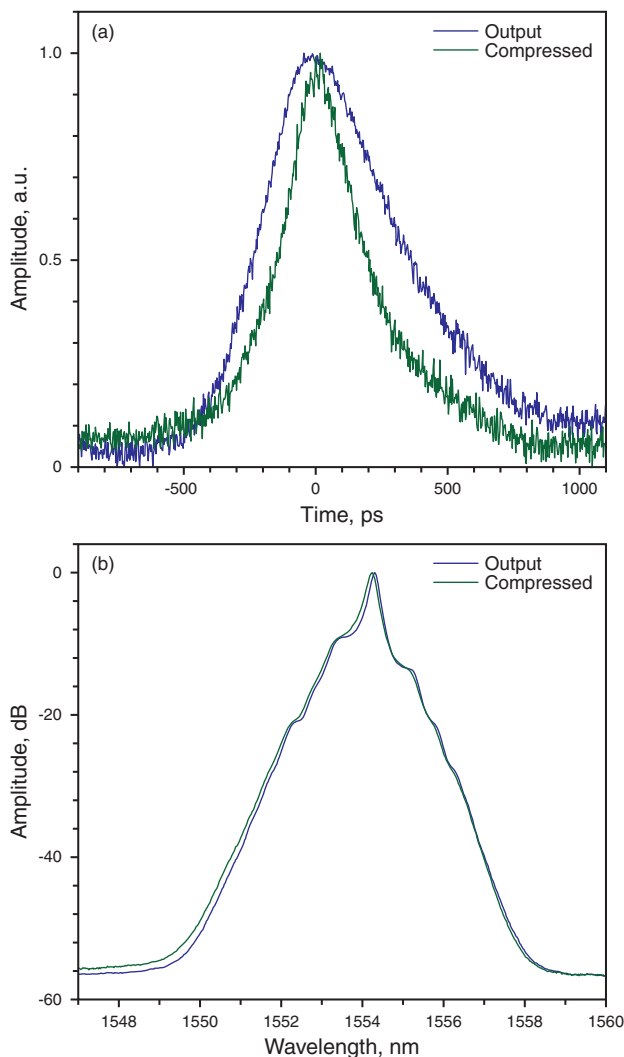


Figure 5 (online color at www.lphys.org) (a) – oscilloscope trace of output 600 ps pulses, from high harmonic mode-locked cavity with 400 m of non-linear fiber, to 350 ps in 21 km of STF and (b) – the optical spectrum before and after compression

pulse was expected to possess a large chirp, indicated by the large time-bandwidth product of 29.8, requiring about 60 km of STF to reach full compression in the ideal situation, assuming a fully linear chirp. Using 21 km of STF with an estimated dispersion of 17 ps/nm/km the pulse should be compressible to 385 ps, which is close to the obtained value of 350 ps, with the discrepancy allowed for the uncertainty on the value of dispersion. Temporal envelopes of both uncompressed and compressed pulses and their optical spectra are shown in Fig. 5. Due to no significant changes in the optical spectra it is typical to assume that compression because of the negative chirp of the STF took place in the absence of significant nonlinear contributions.

4. Conclusion

To summarize, harmonic mode-locking of a Raman laser was demonstrated in several configurations with the use of a few layers of graphene as a saturable absorber. Different pulse durations and pulse shapes, as well as variable repetition rates were obtained depending on polarization, pump power adjustments, filter bandwidth and length of the gain fiber. Not all of these changes were quantitatively controlled and further studies will be carried out to explain more completely the dynamics of this Raman laser. Single pulse operation could also be achieved when the longer lengths of fiber were used and a 600 ps pulse was compressed to 350 ps by 21 km of a STF. The use of an optical filter was shown to be essential to make mode-locking stable. The demonstrated approach of combining Raman gain and the saturable absorption of graphene for mode-locking is a potential technique to develop wavelength versatile ultrashort pulsed sources.

References

- [1] C. Lin, L.G. Cohen, R.H. Stolen, G.W. Tasker, and W.G. French, *Opt. Commun.* **20**, 426–428 (1977).
- [2] J.C. Hernandez-Garcia, O. Pottiez, R. Grajales-Coutiño, B. Ibarra-Escamilla, E.A. Kuzin, J.M. Estudillo-Ayala, and J. Gutierrez-Gutierrez, *Laser Phys.* **21**, 1518–1524 (2011).
- [3] X.H. Li, Y.S. Wang, W. Zhao, W. Zhang, Z. Yang, X.H. Hu, H.S. Wang, X.L. Wang, Y.N. Zhang, Y.K. Gong, C. Li, and D.Y. Shen, *Laser Phys.* **21**, 940–944 (2011).
- [4] M.R.A. Moghaddam, S.W. Harun, R. Akbari, and H. Ahmad, *Laser Phys.* **21**, 913–918 (2011).
- [5] H. Feng, W. Zhao, S. Yan, and X.P. Xie, *Laser Phys.* **21**, 404–409 (2011).
- [6] Y.H. Zhong, Z.X. Zhang, and X.Y. Tao, *Laser Phys.* **20**, 1756–1759 (2010).
- [7] D.A. Chestnut and J.R. Taylor, *Opt. Lett.* **30**, 2982–2984 (2005).
- [8] J. Schröder, S. Coen, F. Vanholsbeeck, and T. Sylvestre, *Opt. Lett.* **31**, 3489–3491 (2006).
- [9] C. Agueraray, D. Méchin, V. Kruglov, and J.D. Harvey, *Opt. Express* **18**, 8680–8687 (2010).
- [10] A. Chamorovskiy, J. Rautiainen, J. Lytykäinen, S. Ranta, M. Tavast, A. Sirbu, E. Kapon, and O.G. Okhotnikov, *Opt. Lett.* **35**, 3529–3531 (2010).
- [11] S. Kivistö, T. Hakulinen, A. Kaskela, B. Aitchison, D.P. Brown, A.G. Nasibulin, E.I. Kauppinen, A. Härkönen, and O.G. Okhotnikov, *Opt. Express* **17**, 2358–2363 (2009).
- [12] E.J.R. Kelleher, J.C. Travers, Z. Sun, A.C. Ferrari, K.M. Golant, S.V. Popov, and J.R. Taylor, *Laser Phys. Lett.* **7**, 790–794 (2010).
- [13] J.C. Travers, J. Morgenweg, E.D. Obratsova, A.I. Chernov, E.J.R. Kelleher, and S.V. Popov, *Laser Phys. Lett.* **8**, 144–149 (2011).
- [14] C.E.S. Castellani, E.J.R. Kelleher, J.C. Travers, D. Popa, T. Hasan, Z. Sun, E. Flahaut, A.C. Ferrari, S.V. Popov, and J.R. Taylor, *Opt. Lett.* **36**, 3996–3998 (2011).

- [15] C.E.S. Castellani, E.J.R. Kelleher, D. Popa, Z.P. Sun, T. Hasan, A.C. Ferrari, S.V. Popov, and J.R. Taylor, in: the European Conference on Lasers and Electro-Optics and the European Quantum Electronics Conference, Munich, Germany, May 22–26, 2011 (CLEO/Europe-EQEC 2011), paper JSII2.2.
- [16] F. Bonaccorso, Z. Sun, T. Hasan, and A.C. Ferrari, *Nat. Photon.* **4**, 611–622 (2010).
- [17] H. Zhang, D.Y. Tang, R.J. Knize, L.M. Zhao, Q.L. Bao, and K.P. Loh, *Appl. Phys. Lett.* **96**, 111112 (2010).
- [18] A.K. Geim and K.S. Novoselov, *Nat. Mater.* **6**, 183–191 (2007).
- [19] H. Zhang, D.Y. Tang, L.M. Zhao, Q.L. Bao, K.P. Loh, B. Lin, and S.C. Tjin, *Laser Phys. Lett.* **7**, 591–596 (2010).
- [20] W.H. Renninger, A. Chong, and F.W. Wise, *Phys. Rev. A* **77**, 023814 (2008).
- [21] E.J.R. Kelleher, J.C. Travers, E.P. Ippen, Z. Sun, A.C. Ferrari, S.V. Popov, and J.R. Taylor, *Opt. Lett.* **34**, 3526–3528 (2009).
- [22] E.J.R. Kelleher, J.C. Travers, Z. Sun, A.G. Rozhin, A.C. Ferrari, S.V. Popov, and J.R. Taylor, *Appl. Phys. Lett.* **95**, 111108 (2009).
- [23] J.-H. Lin, D. Wang, and K.-H. Lin, *Laser Phys. Lett.* **8**, 66–70 (2011).
- [24] J. Fekete, A. Cserteg, and R. Szipőcs, *Laser Phys. Lett.* **6**, 49–53 (2009).
- [25] Z.Q. Luo, T. Yu, J.Z. Shang, Y.Y. Wang, S.H. Lim, L. Liu, G.G. Gurzadyan, Z.X. Shen, and J.Y. Lin, *Adv. Funct. Mater.* **21**, 911–917 (2011).
- [26] N. Papasimakis, Z.Q. Luo, Z.X. Shen, F. De Angelis, E. Di Fabrizio, A.E. Nikolaenko, and N.I. Zheludev, *Opt. Express* **18**, 8353–8359 (2010).
- [27] Z.P. Sun, T. Hasan, F. Torrisi, D. Popa, G. Privitera, F.Q. Wang, F. Bonaccorso, D.M. Basko, and A.C. Ferrari, *ACS Nano* **4**, 803–810 (2010).